Montoya, N.; Montagna, E.; Lee, Y.; Domenech Carbo, MT.; Doménech Carbó, A. (2017). Raman spectroscopy characterization of 10-cash productions from the late Chinese emperors to the Republic. Journal of Raman Spectroscopy. 48(10):1337-1345. doi:10.1002/jrs.5218

Raman spectroscopy characterization of ten-cash productions from the late Chinese emperors to the Republic

Noemí Montoya[a], Elena Montagna[b], Yu Lee[c], María Teresa Doménech-Carbó[b], Antonio Doménech-Carbó*[a]

[a] Departament de Química Analítica. Universitat de València. Dr. Moliner, 50, 46100 Burjassot (València) Spain.
[b] Institut de Restauració del Patrimoni, Universitat Politècnica de València, Camí de Vera 14, 46022, València, Spain
[c] Department. of Cultural Heritage Conservation, National Yunlin University of Science and Technology, 123 University Road, 64002 Yunlin, Taiwan.

* Corresponding author, e-mail: antonio.domenech@uv.es
Tel: + 48 963543157, Fax:+ 34 963544436 ,

Abstract

The use of Raman spectroscopy for discriminating monetary emissions, a recurrent problem in much archaeological studies, is described. The method involves the record of Raman signatures of tenorite and crystalline and defective cuprite in the patina based on the idea that subtle, mint-characteristic variations in the composition and metallography of the base metal during the manufacturing process are reflected in the variation in depth of the composition and crystallinity of the corrosion patina. The technique was applied to a series of ten cash copper coins produced around the transition between the Kuang Hsü and Hsüan T'ung last Chinese emperors and the first Republic whose averaged composition was 95±1 % wt Cu plus 5±1 % wt Zn often accompanied by traces of Sn and Pb. Raman data, corroborated by focusing ion beam-field emission scanning electron microscopy (FIB-FESEM-EDX) and voltammetry of immobilized particles (VIMP) measurements, suggested the possibility of discerning between different provincial and regular unified currency productions.

Keywords: Archaeometry; Mint discrimination; Copper coins; Cuprite; Tenorite.

1. Introduction

The determination of the materials and techniques of production as well as the provenance of archaeological objects is of crucial importance in Archaeometry, conservation and restoration of cultural heritage. In the case of metal objects, metallographic analysis, trace elements content and isotope analysis, among other techniques, are well-established techniques for these analytical targets.[1] Such techniques, which provide fundamental analytical information, also possess limitations, as discussed for isotope analysis [2,3] and x-ray fluorescence.[4] and require in general more or less invasive sampling within the metal core. This is a significant problem in most cases in which the maintenance of the integrity of the object is an essential requirement.[5,6] Accordingly, there is a growing interest in analytical techniques yielding archaeometric information from analytical data taken exclusively from the metal patina.[7-11]

Due to its sensitivity and non-invasive character, Raman spectroscopy is being increasingly used in the study of artistic and archaeological objects.[12] In particular, Raman spectroscopy has been used for identifying corrosion products in copper/bronze and other metals,[13-19] and characterizing artistic patinas produced in copper-base alloys.[20-25]

In this report, we describe the use of Raman spectroscopy for discriminating different monetary emissions. The essential idea was that this analytical target, which can be attained through metallographic, isotope, trace analysis, … techniques involving the processing of the metal nucleus, can complementarily be accessed from non-invasive analysis of the metal patina. For this purpose, it was hypothesized that, when series of objects experiencing a common corrosion conditions was studied, even subtle differences in the composition and/or metallographic structure of the base metal will be reflected in the composition of the corrosion layers and the distribution of the corrosion products through the patina which can be detected by means of Raman spectroscopy. This idea, which is in agreement with previous studies on bronze coins using solid-state electrochemical techniques,[26,27] is consistent with the reported sensitivity of the Raman

spectra of copper oxides, cuprite in particular, to the crystallinity and grain size,[20,29-32] in particular, in thin solid films.[33-35] It has to be noted, however, that the 'corrosion history' experienced by the objects under study may have been considerably different so that the above hypothesis can only be reasonably applied to selected sets of samples.

In a previous report,[27] we applied the voltammetry of immobilized particles (VIMP), an electrochemical technique, for discriminating different series of ten-cash Dragon copper coins minted during the reign of the last Qing Dynasty Chinese Emperors Kuang Hsü (1875-1908) and Hsüan T'ung. This monetary production occurred through drastic political and social changes in China, arising from one of the most chaotic monetary systems in the world.[33] Before 1889, when the Viceroy Ch'ang Ch'ih-tung in Kwangtung Province initiated the production of western type coins, provincial viceroys minted their own local coinage. Although between 1901 and 1906, the emperor Kuang Hsü promoted a unified coinage system,[36] our electrochemical data suggested that the monetary production continued exhibiting certain heterogeneity and permitted to distribute the coins into four electrochemical types associated to different centers of production.[27]

In order to test the above electrochemical screening and study the possibility of the maintenance of a heterogeneous minting during the republican period, Raman spectroscopy was applied to the above and a second series of coins mainly corresponding to the first currency produced by the Republic of China since 1911. The study presented here was conducted from a set of 59 ten-cash copper coins that includes coins of the Regular Provincial series minted in different provinces as well as of the unified Hu Poo and Tai Ching Ti Kuo unified series, all of the imperial period, and Republican currency from different mints whose characteristics are summarized in Table 1 (see also Supplementary information, Table S1). A first sub-series of 38 coins of imperial series was previously studied by means of VIMP and focusing ion beam-field emission scanning electron microscopy (FIB-FESEM-EDX).[27] Here, the entire set of 59 coins (Empire and Republican series) is studied by Raman spectroscopy adding VIMP and FIB-FESEM-EDX data for the sub-set of Republican series.

2. Experimental

2.1. Samples

A total of 59 ten cash Chinese coins from different mints were studied. The legends, denominations and design of the coins are provided in ref. [27] and as a Supplementary information (Table S1).

2.2. Instrumentation and methods

Raman spectra of different coins were obtained by means of a XPlora Horiba MTB model and a 532 nm laser as excitation with maximum power of 90 mW. The samples were measured in backscattering geometry at room temperature. A 100 confocal microscope objective was used to focus the excitation laser on the sample and collect the scattered light to the spectrometer. A minimum of 6 different areas were analyzed per coin, to obtain representative results. Exposure time, number of acquisitions and laser power varied among 5–20 s, 10–50 and 30–80 mW, respectively. Selected conditions for peak area measurements were 15 s of exposure time, 40 acquisitions and laser power 60 mW. Data acquisition was carried out with the LabSpec 6 Spectroscopy Suite from Horiba MTB. For Raman depth measurements, samples were mounted on an *x*,*y* motorized stage, with *z*-displacement controlled with a piezo-transducer on the objective. The confocal pinhole diameter was 200 mm, and the slit width was 100 mm.

Sectioning of coins and imaging of the resulting trench were performed with a FIB-FESEM Zeiss (Orsay Physics Kleindiek Oxford Instruments) model Auriga compact equipment that enabled the characterization of the microtexture and mineral phases in the superficial corrosion layer and in the metal core of the 20th century coins. The operating conditions were: voltage, 30 kV and current intensity, 500µA and 20 nA in the FIB for generating the focused beam of Ga ions, a voltage of 3 kV in the FESEM for photographs and X-ray linescans were performed in the trench operating with a Oxford-X Max X-ray microanalysis system coupled to the FESEM controlled by Aztec software. A voltage of 20 kV and a working distance of 6-7 mm was used. The instrument used has a dual beam system that includes an electron beam and a Ga ion beam. For making the trench the stage, where is placed the coin, is tilted 54º so that the Ga beam impacts perpendicularly to the plane of the vertical wall of the trench. In

parallel, the electron beam is optimally focused for acquiring images. Additionally, the software of the instrument automatically carries out a "tilt compensation" for correcting the secondary electron images

Electrochemical experiments were performed using materials and equipment already described[26,27] (for details, see Supplementary information).

3. Results and Discussion

3.1. Organoleptic properties and composition

The studied coins presented a uniform light brownish patina, rarely showing any minor localized deposit of green corrosion products. The averaged composition of the base metal, determined from FIB-FESEM-EDX experiments (vide infra), was 95±5 % wt Cu plus 5±1 % wt Zn often accompanied by traces of Sn and Pb with minor variations between different mints. Pertinent data are presented as Supplementary information, Table S2. In regard to the uniformity and representativity of the sample, it is pertinent to note that the coins provided originally from a private collection where they were conserved since ca. 1925. Given the relatively low time of circulation of the coins and their uniform conditions of storage, the studied set of coins appeared as reasonably uniform in regard to the conditions required for mint discrimination described in the Introduction section. On the other hand, all coins were of types widely circulated in the studied historical period (no unusual currency[36] was tested) so that they can in principle be considered as reasonably representative of the currency production by the different mints.

3.2. Raman spectra

Figure 1 compares the Raman spectra of cuprite and tenorite with that of coin Peiyang #01. The spectrum of cuprite shows two main bands at 114 and 220 cm^{-1}, accompanied by shoulders at 145 and 186 cm^{-1}, which are in agreement with literature data.[13-25] Weak, broad bands also appear at 420, 525 and 625 cm^{-1}.[29-35,37,38] These last bands can be assigned to Cu_2O amorphous or finely divided,[31] and characterize defective cuprite forming native passive layer on copper/bronze objects.[21,30,31] The spectrum of tenorite

was dominated by the band at 297 cm^{-1}, accompanied by weak signals at 346 and 631 cm^{-1}, also in agreement with literature.[33,34,39]

In a first series of experiments, the spectra of Chinese ten-cash coins were recorded on at least 6 different regions on each coin in order to obtain information on the composition of the external surface of the coin. Although obscured by background fluorescence, such spectra presented well-defined cuprite bands at 90 and 215 cm^{-1}, accompanied by signals at 145, 525 and 620 cm^{-1}.[21-25] The principal tenorite band at 297 cm^{-1} was weak or almost absent while the signal at 631 cm^{-1} possibly appeared as broadening the cuprite band at 625 cm^{-1}. On comparing the spectrum of microcrystalline cuprite in Figure 1a with the spectrum of coins (Figure 1c), one can see that the height of the signals at 525 and 625 cm^{-1}, characterizing the cuprite passive layer formed onto copper surfaces,[21,30,31] is clearly enhanced in the spectra of the studied coins. The spectra recorded in different spot of the same coin presented in general high concordance, with deviations in the Raman shift of peaks of ±1 cm^{-1} and in the intensity ratio between the different bands below ±5 %.

In order to test possible systematic differences between the studied coins, the areas of cuprite bands at 90 and 215 cm^{-1} were determined. Peak intensity measurements were also carried out using the base line depicted in Figure 2 in which three spectra recorded on different spots of coin Anhui RG#01 are shown. As can be seen in this figure, the Raman spectra, although maintaining a common general profile, exhibit differences in the absolute values of the areas. This feature can be attributed to the differences in optical path resulting from local differences in the composition, roughness, etc. of the coin surface. Our data indicated, however, that the peak area ratio between bands at 90 and 215 cm^{-1}, A_{90}/A_{215}, varied systematically with each one of the absolute values of these areas. This feature can be interpreted on assuming that the respective areas are representative of the crystallinity of cuprite which in turn varies with depth (*vide infra*) in the patina of the coins. Accordingly, depending on the local optical path, the Raman spectrum will be representative of more or less deep corrosion layers so that the A_{90}/A_{215} should vary with A_{90} and A_{215} according to a law depending on the depth variation of

composition, a situation parallel to that discussed for the variation of the tenorite/cuprite ratio determined from voltammetric data.[27]

Data corresponding to late imperial currency are depicted in Figure 3 where the ratio of the peak areas for bands at 90 and 215 cm^{-1}, A_{90}/A_{215}, is plotted as a function of the absolute area of the band at 90 cm^{-1}. In this figure, four of the six data points taken for each coin have been represented; for simplicity, the upper and lower extreme values of each coin have been removed. Error bars correspond to the standard deviations estimated for the peak area measurements, with averaged values of 5% for peak areas and 7% for the peak area ratio.

In this representation one can see that experimental data points for imperial series are grouped into four groups (labeled from I to IV) corresponding to: group I: Tai Ching Ti Kuo #01 to #11; group II: Hupeh and Anhwei provincial coins; group III: Honan and Kiangnan provincial series and Hu Poo unified series; group IV; Hunan and Kwantung provincial series. Remarkably, Raman grouping was entirely coincident with that previously performed using VIMP data previously reported.[27] Similar results were obtained using peak intensities.

3.3. Electron microscopy analysis

To explore the reasons for the observed differences in the Raman spectra of coins from different series, FIB-FESEM-EDX experiments using a Ga ions microbeam were performed. This micro-invasive technique permits to perform trenches of 10 x 10 μm by means of a ionic microbeam no detectable at the macroscopic level. Figure 4 shows the secondary electron images of trench *ca.* 10 μm length and *ca.* 15 μm depth generated by FIB in the region of interest in the coins: a) Fukien #01 (Regular Provincial series); b) Tai Ching Ti Kuo #12; c) Honan #01; d) Kiangnan RG#01 (Republican). The trenches are extended from the outer corrosion layers down to the metal core of the coin showing clear differences in the thickness and texture of the corrosion layer which can easily be seen in the upper region and in the grained microtexture of the metal core where microdomains of different shape and size can be distinguished. Such differences can be

attributed to differences in the composition of the base alloy and in its metallographic structure, in turn depending on the thermomechanical treatment used for the production of the coin.

This second aspect appears to be crucial as denoted by EDX analysis coupled to FIB-FESEM imaging. The composition of the metal core was exclusively of Cu and Zn being averaged to 95±1 % wt Cu plus 5±1 % wt Zn, in agreement with literature.[36] Representative compositions are presented as Supplementary information (Table S2). No aggregates of Pb nor Sn were detected. Pertinent data are presented as Supplementary material (Figure S3). The percentage of copper varied differently with depth *z* for the different series of coins. For coins from the regular provincial series, In contrast with the uniformity of the composition of the metallic nucleus, the external regions of the coins showed significant differences which can in principle be attributed to the different environmental attack suffered by individual coins, but also to differences in corrosivity of the metal derived from their different metallographic structure iin turn resulting from possible differences in the raw material, dosification and, mainly, the thermomechanical process used in the fabrication of the coins.

3.4. In depth analysis of Raman data

Figure 5 depicts a series of spectra recorded on coin Hunan RG #01 at different depths. One can see that the relative intensity of bands characterizing crystalline cuprite (C), defective cuprite (C_d) and tenorite (T) varies with depth. These variations are provided as a Supplementary information (Figure S4). In agreement with previous considerations, the ratio between the signal for defective cuprite, associated to the primary corrosion patina, and crystalline cuprite, A_{625}/A_{215} (and I_{625}/I_{215}), decreases in the external region whereas the tenorite/cuprite ratio, given by the A_{295}/A_{215} (and I_{295}/I_{215}) ratio, increases from the primary patina to the external region, further decreasing in the more external layers. This last feature can be attributed to failure in focalization or to the existence of a compromise between the rates of oxygen permeation and cuprite to tenorite oxidation in the corrosion layers.

These features can be interpreted on considering that, as described by Robbiola et

al.,[3-5] under 'ordinary' atmospheric corrosion, copper-based objects form a primary patina of cuprite subsequently growing and forming a more permeable secondary patina whose composition will be dependent on the type of environmental attack so that copper corrosion patinas should be viewed as stratified systems where composition gradients exist. Accordingly, as will be treated in detail below, that the absolute intensity of the Raman bands increases as the effective excitation increases and that, at the same time, the depth of the Raman-responsive region in the patina of the coins increases. Then, the variations in the relative intensity of the bands will reflect the in depth variation of the composition and crystallinity of the cuprite patina.

3.5. Correlation with voltammetric data

The foregoing set of considerations are consistent with voltammetric data obtained for samples of the patina of the coins transferred onto graphite electrodes in contact with air-saturated aqueous acetate buffer at pH 4.50. Pertinent data are presented as Supplementary materials in Figure S1. Sampling on the patina of the coins, voltammetric signals for the reduction of cuprite (Cu_2O) at ca. –0.10 V (C_1) and tenorite CuO) ca. –0.35 V (C_2) were recorded so that the variation between the ratio of peak currents for tenorite and cuprite reduction processes, $i_p(C_2)/i_p(C_1)$, varied systematically on $i_p(C_1)$ as depicted in Figure S2 (Supplementary materials). All data points were grouped in a band roughly corresponding to a potential variation of the $i_p(C_2)/i_p(C_1)$ on $i_p(C_1)$ which is in agreement with data for provincial and imperial series previously studied,[27] allowing to grouping the coins in four electrochemical types (labeled from I to IV). This grouping can be rationalized taking into account that the conversion of cuprite into tenorite in contact with a O_2-rich atmosphere is a thermodynamically spontaneous process,[40,41] so that the tenorite/cuprite ratio should increase from the deep to the more external corrosion layers.[27]

Voltammetric data for late imperial and Republican ten-cash series studied here, fall within the band attributable to the electrochemical type III in Figure S2. Interestingly, Raman spectroscopy data provided a refined grouping of such coins. As shown in Figure 6, where the variation of the ratio between the areas of peaks at 90 and 215 cm^{-1},

A_{90}/A_{215}, are plotted as a function of the values of A_{215}, data points can be assigned to three tendency lines corresponding to: i) Republican coins (including both general use and commemorative subseries in Table 1); ii) Tai Ching Ti Kuo #12 and #13; iii) Honan and regular provincial series from Chekiang, Fukien and Peiyang. These series define three Raman types appearing as sub-divisions of the electrochemical type III.

3.6. Archaeometric implications

In order to extract archaeometric information, it has to be emphasized that the composition and metallographic properties of the base metal are the essential data to be acquired for discriminating different monetary emissions. Given the heterogeneity and variety of conditions of aging experienced by the coins, the methodologies addressed to avoid invasive sampling based on the analysis of the patina, have high inherent limitations and can only be applied under favorable conditions to samples for which common conditions of aging can be assumed.

The obtained Raman grouping can be summarized as:

a) The coins of imperial series were distributed into four groups (labeled from I to IV in Figure 3) coincident with those previously proposed on the basis of independent VIMP measurements.[27] The Regular Provincial series were grouped according a well-defined geographical distribution discriminating between coins minted in the central provinces (Hupeh and Anhwei, type II), the northern-central provinces of Honan, Kiangnan and Kiangsi (type III) and southern provinces (Hunan and Kwantung, type IV).

b) The two series of unified currency fabricated in the imperial era were distributed in two groups, the gross of the Tai Ching Ti Kuo series (Tai Ching Ti Kuo #01 to #11) formed a different group (type I).

c) The series containing the legend Hu Poo and Tai Ching Ti Kuo coins from Chinkiang and Honan (Tai Ching Ti Kuo #12 and #13) were assigned to the type III (type III-1). A reasonable hypothesis is that such coins were produced in a provincial mint retaining local practice.

d) Republican coins of the General use and Commemorative sub-series from the different mints formed a homogeneous group near the previous Raman type III (type

III_2) while imperial coins from the Regular Provincial series minted in Chekiang, Fukien and Peiyang formed a third Raman group (type III-3) characterized by low A_{90}/A_{215} ratios, coincident with Republican coins of the Regular provincial sub-series from Honan. All these coins produced a similar VIMP response (see Supplementary materials, Figure S2).

It is pertinent to underline that the above Raman grouping was correlated with numismatic data as far as all coins of the same mint were of the same Raman group, and that this grouping was coincident with electrochemical grouping of the same samples using an entirely independent set of experimental data.

The above data indicate that, in spite of the aforementioned limitations, the monetary unification was not made effective until the creation of the Republic of China, confirming prior data based on a different set of coins of imperial time, suggesting that the production of unified currency, ideally initiated with the Hu Poo and Tai Ching Ti Kuo series, was not entirely performed.[27] Raman data indicate that, although displaying a common electrochemical pattern (type III) there were differences in the coin production between the late imperial Regular Provincial series, the unified imperial currency (Tai Ching Ti Kuo series) and the Republican production and that even in this last period some currency (Honan series) was minted following provincial uses.

4. Conclusions

Application of Raman spectroscopy to a series of ten cash coins of the provincial series, unified imperial emissions and Republic of China series permits to detect features characterizing the presence of tenorite and different cuprite forms in the corrosion patina. The depth variation of the relative intensity of bands for the different cuprite forms was consistent with the expected variation in crystallinity from the primary and secondary patina of the coins. The differences in the variation of the above Raman integrated intensities can tentatively be considered as representative of the light differences in the production mode. Grouping of coins based on the ratio of peak areas

of cuprite bands was coincident with that derived from electrochemical data, thus suggesting that there is possibility of discriminating between different mints. As a result, one can conclude that provincial, local production types of currency were maintained, contrary to the presumed monetary unification carried out in this period, during the late empire, and that the unified production of currency was effective only in the Republic of China emissions. All these results indicate the possibility of using Raman spectroscopy as a complementary tool for discriminating monetary emissions of application in numismatic and archaeological studies.

Acknowledgements. Financial support from the MINECO Projects CTQ2014-53736-C3-1-P and CTQ2014-53736-C3-2-P which are also supported with ERDF funds. The authors also wish to thank the Prehistory Museum of Valencia and Dr. José Luis Moya López and Mr. Manuel Planes Insausti (Microscopy Service of the Universitat Politècnica de València) for technical support.

References

[1] D. Attanasio, G. Bultrini, G.M Ingo, *Archaeometry* **2001**, *43*, 529.

[2] P. Budd, D. Gale, A. M. Pollard, R. G. Thomas, P. A. Williams, *Archaeometry* **1993**, *35*, 241.

[3] T. H. Rehren, E. Pernicka, *Archaeometry* **2008**, *50*, 232.

[4] R. Linke, M. Schreiner, G. Demortier, M. Alram, *X-Ray Spectrom*. **2003**, *32*, 373.

[5] D. A. Scott, *J. Amer. Ite. Conservat*. **1994**, *33*, 1.

[6] L. Robbiola, J. M. Blengino, C. Fiaud, *Corros. Sci*. **1998**, *40*, 2083.

[7] L. Robbiola, R. Portier, *J. Cult. Herit*. **2006**, *7*, 1.

[8] C. Chiavari, K. Rahmouni, H. Takenouti, S. Joiret, P. Vermaut L. Robbiola, *Electrochim. Acta* **2007**, *52*, 7760.

[9] I. Constantinides, A. Adriaens, F. Adams, *Appl. Surf. Sci*. **2002**, *189*, 90.

[10] I. De Ryck, A. Adriaens, E. Pantos, F. Adams, *Analyst* **2003**, *128*, 1104.

[11] M. C. Bernard, S. Joiret, *Electrochim. Acta* **2009**, *54*, 5199.

[12] J. M. Madariaga, D. Bersani, Eds. *Raman spectroscopy in art and archaeology*, *J. Raman Spectrosc*. Special issue, **2012**.

[13] R. L. Frost, *Spectrochim. Acta A* **2003**, *59*, 1195.

[14] M. Bouchard, D. C. Smith, *Spectrochim. Acta A* **2003**, *59*, 2247.

[15] V. Hayez, J. Guillaume, A. Hubin, H. Terryn, *J. Raman Spectrosc*. **2004**, *35*, 732.

[16] V. Hayez, T. Segato, A. Hubin, H. Terryn, *J. Raman Spectrosc*. **2006**, *37*, 1211.

[17] P. Colomban, A. Tournié, M. Maucuer, P. Meynard, *J. Raman Spectrosc*. **2012**, *43*, 799.

[18] F. Ospitali, C. Chiavari, C. Martini, E. Bernardi, F. Passarinic, L. Robbiola, *J. Raman Spectrosc*. **2012**, *43*, 1596.

[19] I. Żmuda-Trzebiatowska, K. Schaefer, A. Sokołowska, I. Rodzik, A. T. Sobczyk, J. Karczewskic, G. Śliwińskia, *J. Raman Spectrosc*. **2016**, *47*, 1528.

[20] P. Ropret, T. Kosec, *J. Raman Spectrosc* **2012**, *43*, 1578.

[21] V. Bongiorno, S. Campodonico, R. Caffara, P. Piccardo, M. M. Carnasciali, *J. Raman Spectrosc*. **2012**, *43*, 1617.

[22] G. Bertolotti, D. Versan, P. P. Lottici, M. Alesiani, T. Malcherek, J. Schlüter, *Anal. Bioanal. Chem*. **2012**, *402*, 1451.

[23] A. C. Municchia, F. Bellatreccia, G. D'Ercoli, S. Lo Mastro, I. Reho, M. A. Ricci, A. Sodo, *Appl. Phys. A* **2016**, *122*, 1021.

[24] M. A. Bouchard, *Numismat. Change* **1999**, *299*, 29.

[25] I. R. Lewis, H. Edwards, *Handbook of Raman Spectroscopy: From the Research Laboratory to the Process Line*, Marcel Dekker, New York, **2001**.

[26] F. Di Turo, N. Montoya, J. Piquero-Cilla, C. De Vito, F. Coletti, G. Favero, A. Doménech-Carbó, *Anal. Chim. Acta* **2017**, *955*, 36.

[27] A. Doménech-Carbó, M. T. Doménech-Carbó, E. Montagna, C. Álvarez-Romero, Y. Lee, *Talanta* **2017**, *169*, 50.

[28] H. Y. H. Chan, C. G. Takoudis, M. J. Weaver, *J. Phys. Chem. B* **1999**, *103*, 357.

[29] G. Niaura, *Electrochim. Acta* **2000**, *45*, 3507.

[30] M. Serghini-Idrissi, M. C. Bernard, F. Z. Harrif, S. Joiret, K. Rahmouni, A. Srhiri, H. Takenouti, V. Vivier, M. Ziani, *Electrochim. Acta* **2005**, *50*, 4699.

[31] E. Basso, C. Invernizzi, M. Malagodi, M. F. La Russa, D. Bersani, P. P. Lottici, *J. Raman Spectrosc*. **2014**, *45*, 238.

[32] C.J. Keturakis, B. Notis, A. Blenheim, A.C. Miller, R. Pafchek, M.R. Notis, I.E. Wachs, *Appl. Surf. Sci*. **2016**, *376*, 241.

[33] W. Ning, C. Xia, C. Xiaolan, X. Yanjun, G. Lin, *Analyst* **2010**, *135*, 2106.

[34] H. Stein, D. Naujoks, D. Grochla, C. Khare, R. Gutwoski, S. Grützke, W. Schuhmann, A. Ludwig, *Phys. Status Solidi A* **2015**, *212*, 2798.

[35] L. Coelho, J. A. Moreira, P. B. Tavares, J. L. Santos, D. Viegas, J. M. M. M. de Almeida, *Sens. Actuat. A* **2017**, 253, 69.

[36] A.M. Tracey Woodward, The minted ten-cash coins of China, M.R. Fried Publ. Oakland, **1971**.

[37] A. Nath, A. Khare, *J. Appl. Phys*. **2011**, 110, 043111.

[38] N. Welter, U. Schüssler, W. Kiefer, *J. Raman Spectrosc*. **2007**; 38; 113.

[39] L. Debbichi, M. C. Marco de Lucas, J. F. Pierson, P. Krüger, *J. Phys.Chem. C* **2012**; *116*, 10232.

[40] D. A. Scott, *Stud. Conservat*. **1997**; 42, 93.

[41] M. T. S. Nair, L. Guerrero, O. L. Arenas, P. K. Nair, *Appl. Surf. Sci*. **1999**; 150, 143.

Table 1. Summary of historical and numismatic data for coins in this study.

Reference	Date/Period	Mintmark	Mint
Imperial Regular Provincial Series			
Anhwei #01	Kuang Hsü period	Anhwei	Anking
Chekiang #01- #04	1903-1906	Chekiang	Hangchow
Fukien #01	Kuang Hsü period	Fukien	Foochow
Honan #01 - #02	Kuang Hsü period	Honan	K'ai-feng Fu
Hunan #01 - #03	Kuang Hsü period	Hunan	Changsha
Hupeh #01 - #02	Kuang Hsü period	Hupeh	Wuchang
Kiangnan #01 - #04	1902, 1904, 1905	Kiangnan	Nanking
Kwantung #01 - #03	Kuang Hsü period	Kwantung	Canton
Peiyang #01	Kuang Hsü period	Peiyang	Peiyang (Tientsin)
Imperial Unified series			
Hu Poo #01 - #06	Kuang Hsü period	Hu Poo	Peiyang
Tai Ching Ti Kuo #01	1906	Hupeh	Wuchang
Tai Ching Ti Kuo #02	1905	Hu Poo	Peiyang
Tai Ching Ti Kuo #03	1907	Hu Poo	Peiyang
Tai Ching Ti Kuo #04	1906	Anhwei	Anking
Tai Ching Ti Kuo #05	1906	Hupeh	Wuchang
Tai Ching Ti Kuo #06	1906	Hunan	Changsha
Tai Ching Ti Kuo #07	1906	Hupeh	Wuchang
Tai Ching Ti Kuo #08	1909	Szechwan	Ssûch'uan
Tai Ching Ti Kuo #09	1905	Hu Poo	Peiyang
Tai Ching Ti Kuo #10	1906	Kiangnan	Nanking
Tai Ching Ti Kuo #11	1907	Kiangnan	Nanking
Tai Ching Ti Kuo #12	1906	Chinkiang	Tsin-kiang Pu
Tai Ching Ti Kuo #13	1906	Honan	K'ai-feng Fu
Republic of China Series			
General Use sub-series			
Anhwei_RG #01 and #02	1918, 1921	Anhwei	Anking
Kiangnan_RG #01	After 1911	Kiangnan	Nanking
Hunan_RG #01- #03	After 1911	Hunan	Changsha
Shansi_RG #01	After 1919	Shansi	Tai-yuan Fu
Commemorative sub-series			
Kiangnan_RC #01 and #02	1911	Kiangnan	Nanking
Regular Provincial sub-series			
Honan_RR #01 and #02	After 1911	Honan	K'ai-feng Fu

Figures

Figure 1. Raman spectra of a) cuprite, b) tenorite and c) coin Peiyang #01.

Figure 2. Detail of the low wavenumber region of the Raman spectra of Chinese ten cash coins. Three replicate spectra recorded for coin Anhwei_RG #01 (Republican series) are superimposed. Inset: photographic image of the obverse (left) and reverse (right) of the coin.

Figure 3. Variation of the ratio between the areas of peaks at 90 and 215 cm^{-1}, A_{90}/A_{215} on the area of the first band, A_{90}, recorded in Raman spectra of coins in this study. Experimental data points for coins from Tai Ching Ti Kuo #01 to #11 (solid rhombs), Hupeh and Anhwei Imperial Regular Provincial series (squares), Honan and Kiangnan Imperial Regular Provincial series and Hu Poo Imperial Unified series (solid squares) and Hunan and Kwantung Imperial Regular Provincial series (triangles). Continuous lines represent tendency lines fitting data points to potential laws.

Figure 4. Secondary electron images of trench *ca.* 10 µm length and *ca.* 15 µm depth generated by FIB in the region of interest in the coins: a) Fukien #01 (Republican Regular Provincial series); b) Tai Ching Ti Kuo #12; c) Honan_RR #01 (Republican Regular Provincial series) ; d) Kiangnan_RC #01 (Republican Commemorative series).

Figure 5. Raman spectra of coin Hunan_RG #01(Republican General Use series) at different depths. The bands characterizing crystalline cuprite (C), defective cuprite (C_{df}) and tenorite (T) are marked by arrows.

Figure 6. Variation of the ratio between the areas of peaks at 90 and 215 cm^{-1}, A_{90}/A_{215} on the area of the first band, A_{90}. Experimental data points for coins from: Republican General Use series (squares), Tai Ching Ti Kuo #12 and #13 (solid squares) and Imperial Regular Provincial series minted in Chekiang, Fukien and Peiyang (triangles). Continuous lines represent tendency lines fitting data points to potential laws.

Figure 1.

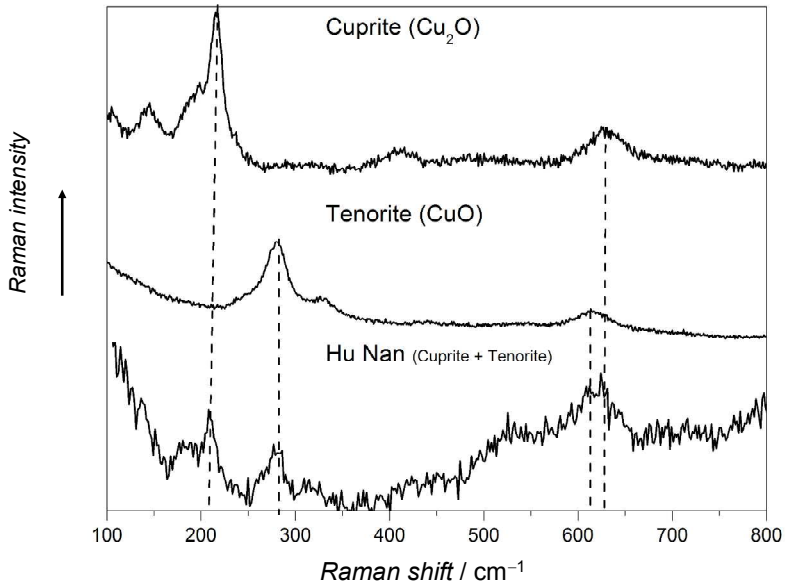

Figure 2.

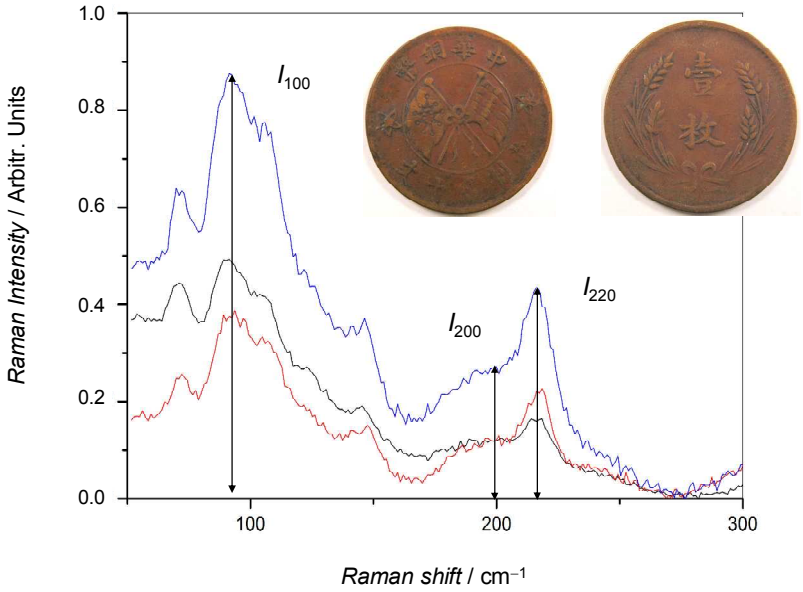

Figure 3.

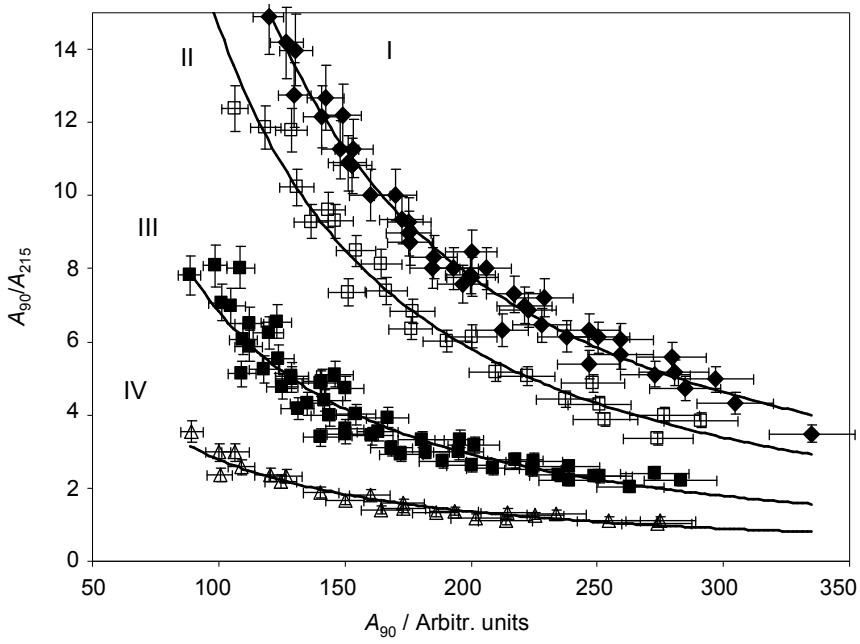

Figure 4.

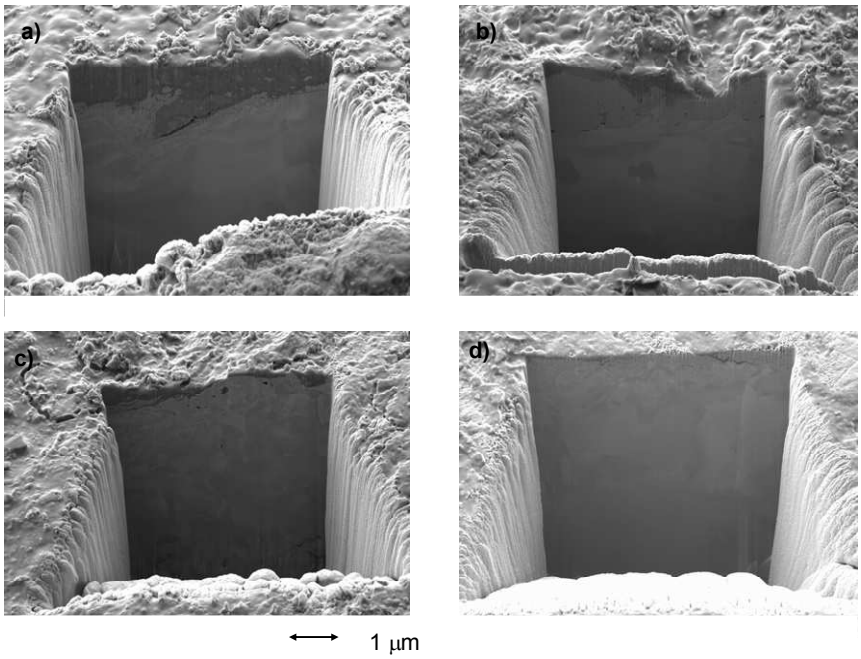

Figure 5.

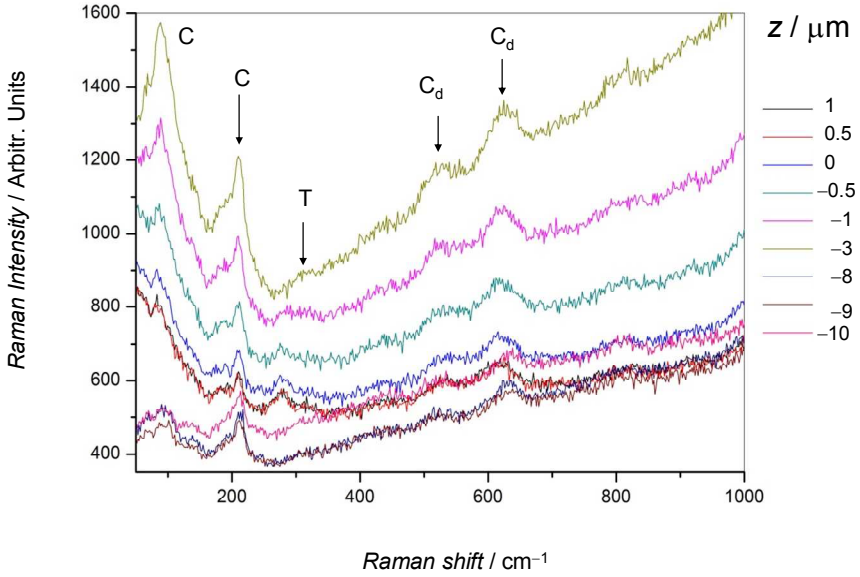

Figure 6.